# On the dynamics of high Rydberg states of large molecules

Joshua Jortner and M. Bixon
*School of Chemistry, Tel Aviv University, Ramat Aviv, 69978 Tel Aviv, Israel*

(Received 20 July 1994; accepted 14 December 1994)

In this paper we explore the level structure, the optical excitation modes and the dynamics of a mixed Stark manifold of very high Rydberg states (with principal quantum numbers $n=80-250$) of large molecules, e.g., 1,4 diaza bicyclo [2,2,2] octane (DABCO) and *bis* (benzene) chromium (BBC) [U. Even, R. D. Levine, and R. Bersohn, J. Phys. Chem. **98**, 3472 (1994)] and of autoionizing Rydbergs of atoms [F. Merkt, J. Chem. Phys. **100**, 2623 (1994)], interrogated by time-resolved zero-electron kinetic energy (ZEKE) spectroscopy. We pursue the formal analogy between the level structure, accessibility and decay of very high Rydbergs in an external weak ($F\simeq 0.1-1$ V cm$^{-1}$) electric field and intramolecular (interstate and intrastate) relaxation in a bound molecular level structure. The onset $n=n_M$ of the strong mixing (in an external field $F$ and in the field exerted by static ions) of a doorway state, which is characterized by a low azimuthal quantum number $l$, a finite quantum defect $\delta$, and a total nonradiative width $\Gamma_s\simeq\Gamma_0/n^3$, with the inactive high $l$ manifold is specified by $n_M\simeq 80.6\,\delta^{1/5}(F/\text{V cm}^{-1})^{-1/5}$. At $n\geqslant n_M$ the level structure and dynamics are characterized by the product $\gamma\rho$, where $\rho$ is the density of states and $\gamma=\Gamma_s D(n)$ is the average decay width of the eigenstates, with the dilution factor $D(n)\approx n^{-2}$ for $(lm_l)$ mixing and $D(n)\simeq n^{-1}$ for $(l)$ mixing, whereupon $\gamma\rho=(\Gamma_0/4\,\delta R)(n_M/n)^5$, being independent of $D(n)$. The sparse level structure is realized for $\gamma\rho\ll 1$, while the dense level structure prevails for $\gamma\rho>1$, resulting in two limiting situations; (a) a dense limit for $n\geqslant n_M$ and a sparse limit for $n\gg n_M$, and (b) a sparse limit for all $n\geqslant n_M$. The experimental information currently available on the decay dynamics of molecular (DABCO and BBC) and atomic (Ar) Rydbergs for $n\geqslant n_M$ corresponds to case (b). The time-resolved dynamics was characterized in terms of the excited state total population probability $P(t)$ and the population probability $I(t)$ of the doorway state. $P(t)$, which is interrogated by time-resolved ZEKE spectroscopy, will exhibit for both the sparse and dense level structures and for all excitation conditions a superposition of exponential temporal decay terms with an average lifetime of $\sim\hbar/\gamma$. $I(t)$ can be used to interrogate coherence effects, which in case (b) are manifested in quantum beats, while case (a) corresponds to a giant resonance with a molecular time characterized by the reciprocal energetic spread of the Stark manifold. The experimental data for the onset of strong mixing and for the diluted lifetimes [$\hbar/\Gamma_s D(n)$ with $D(n)\sim n^{-1}$] of the high Rydbergs ($n\sim 100-200$) of BBC and of DABCO are in accord with the predictions of the theory for the limit of strong $(l)$ mixing. While strong mixing is realized for $F=Fn^5/3.4\times 10^9\delta>1$, we expect that for the weak mixing regime ($F<1$) the dynamics of ultrahigh Rydbergs will be characterized by two distinct ($\sim$ns and $\sim\mu$s) time scales. Finally, we emphasize the universality of the model, which provides a unified description of the level structure and dynamics of high Rydbergs of molecules and of autoionizing atoms. © *1995 American Institute of Physics.*

## I. HIGH RYDBERGS AND ZEKE RYDBERGS

During the development of the theory of intramolecular coupling and dynamics in isolated molecules[1,2] it was recognized[2–4] that the internal conversion rates of low ($n=3-5$, where $n$ is the principal quantum number) Rydberg states of aromatic molecules (as inferred from line broadening[4]) are considerably slower (i.e., by 1–2 orders of magnitude) than those of the intravalence electronic excitations in the same energy domain. The decay channels of low Rydbergs of large aromatic molecules involve both "nonreactive" internal conversion, with a partial width $\Gamma_{\text{IC}}$, which is dominated by the Rydberg$\rightarrow S_n^+\rightarrow S_1^+$ relaxation[5] (where $^+$ denotes high vibrational excitations), and possibly also "reactive" predissociation channels with a partial width $\Gamma_D$. Quantitative data on Lorentzian line broadening of Rydberg states of benzene explored by two-photon spectroscopy for the $nR_g$ series, $n=3-7$ [with total widths $\Gamma(n)=80$ cm$^{-1}$ for $n=3$ and $\Gamma(n)<8$ cm$^{-1}$ for $n=6$],[6] and by one-photon jet spectroscopy for the $3R_u$ [with a total width $\Gamma(3)=34$ cm$^{-1}$],[7] reveal that the lifetimes $\tau(n)$ of these Rydbergs are $\tau(n)=\hbar/\Gamma(n)$, where

$$\Gamma(n)=\Gamma_{\text{IC}}(n)+\Gamma_D(n) \tag{1.1}$$

increase superlinearly with increasing the principal quantum number $n$. The well known $n^{-3}$ scaling law,[8–14] which was originally developed for vibrational ($\Gamma_{\text{VA}}$) and rotational ($\Gamma_{\text{RA}}$) autoionization[8–13] whose widths are $\Gamma_{\text{VA}}\propto n^{-3}$ and $\Gamma_{\text{RA}}\propto n^{-3}$, is also applicable to predissociation,[14] i.e., $\Gamma_D(n)\propto n^{-3}$, and for internal conversion[15] with $\Gamma_{\text{IC}}(n)\propto n^{-3}$. One expects that the total width of a molecular Rydberg, Eq. (1.1), is

$$\Gamma(n)\simeq\Gamma_0/n^3 \tag{1.2}$$

and the lifetimes are

$$\tau(n)=(\hbar/\Gamma_0)n^3, \tag{1.3}$$

 0021-9606/95/102(14)/5636/11/$6.00 

where $\Gamma_0$ is a numerical constant. The energies of the Rydberg states, which are characterized by the lifetimes (1.1)–(1.3), are

$$E(n)=\mathrm{IP}-\frac{R}{(n-\delta_l)^2}, \tag{1.4}$$

where $R$ is the Rydberg constant, IP is the ionization potential, and $\delta_l$ is the quantum defect (which depends on the azimuthal quantum number $l$). Equations (1.2) and (1.3) are approximate as they do not include interchannel mixing.[11,13] Nevertheless these relations serve as a useful overall description. Even, Levine, and Bersohn[15] have reported the lifetimes (obtained from line broadening) of a long Rydberg series of large molecules, i.e., $n=10-30$ of *bis*(benzene) chrominum (BBC) [where $\Gamma(n)=\Gamma_{\mathrm{IC}}(n)+\Gamma_D(n)$], and $n=11-40$ of the vibrationally excited 1,4 diaza bicyclo [2,2,2] octane (DABCO) [where $\Gamma(n)=\Gamma_{\mathrm{VA}}(n)+\Gamma_{\mathrm{IC}}(n)+\Gamma_D(n)$], demonstrating that a scaling law, i.e., $\tau(n)\propto n^{\alpha}$ and $\Gamma(n)\propto n^{-\alpha}$, is well obeyed (with $\alpha=2.6\pm0.2$), being close to the $n^3$ scaling inferred from the approximate relations (1.2) and (1.3). This significant quantification of the overall decay dynamics of molecular Rydbergs ($n<40$) in conjunction with the $n^3$ scaling law, allows for estimates of the lifetime of a very high (e.g., $n=100$) Rydberg to be $\tau(100)\sim5$ ns. This prediction is not borne out by recent experiments[15–18,19(e),19(f)] using zero-electron kinetic energy (ZEKE) spectroscopy.[19,20] The application of time-resolved ZEKE spectroscopy[15–18,19(e),19(f)] to interrogate the lifetimes of ultrahigh ($n\simeq80-250$) molecular and atomic Rydberg states (which will be referred to as ZEKE Rydbergs) provided the following novel information on the experimental front:

(1) Long lifetimes of ZEKE Rydbergs of NO. Reiser *et al.*[19(b)] have observed high lying (within $\sim10\ \mathrm{cm}^{-1}$ below the ionization potential), very long lived ($\sim\mu$s lifetimes) Rydbergs of NO. Chupka[21] pointed out that the lifetimes of these states are considerably longer than expected on the basis of $n^3$ scaling for the predissociative $p$ series of NO.

(2) The lifetime lengthening of molecular ZEKE Rydbergs. The lifetimes of the ZEKE Rydbergs ($n\sim80-250$) of large molecules[15–18,19(e),19(f),21–23] are longer by several (2–4) orders of magnitude than those expected on the basis of the $n^3$ scaling relations. Even, Levine, and Bersohn[15] have established that the lifetimes of ZEKE Rydbergs ($n\gtrsim80$) of BBC and of DABCO are longer by 2–3 orders of magnitude than those expected on the basis of Eq. (1.3), exhibiting a dramatic break in the $\tau(n)$ vs $n$ relation between the lower ($n=10-50$) Rydbergs interrogated by energy-resolved line broadening and the high ($n=80-250$) Rydbergs explored by time-resolved ZEKE spectroscopy. The lifetimes $\tau_Z(n)$ of ZEKE Rydbergs can be empirically expressed by

$$\tau_Z(n)\ =\ (\hbar/\Gamma_0)n^3/D(n), \tag{1.5}$$

where $D(n)$ ($\ll1$) is a dilution factor. The accurate $n$ dependence of $D(n)$ cannot be yet determined, but the experimental data[15] indicate that $D(n)\propto n^{-\beta}$ with $\beta=1-2$.

(3) The universality of the lifetime lengthening of ZEKE Rydbergs. The lengthening effect is manifested for internal conversion, predissociation and autoionization in large molecules,[15–18] for predissociation in diatomic molecules[21–23] and for autoionization in atoms.[24]

(4) The independence of $\tau_Z(n)$ on the external pressure.[16,18]

(5) The dependence of $\tau_Z(n)$ on the laser fluence.[18]

(6) The reduction of $D(n)$ for NO predissociation[23] and for the autoionization of Ar (Ref. 24) by the increase of a homogeneous dc electric field.

## II. MODELS FOR THE LIFETIMES OF ZEKE RYDBERGS

The fascinating novel characteristics of ZEKE Rydbergs triggered interesting theoretical activity, which falls within the framework of two models.

(a) The Rydberg electron-core rotation model. Levine, Rabani, and Even[15,25,26] have proposed that for ZEKE Rydbergs all the intramolecular decay channels considered above are switched off and Rydberg-core rotation coupling dominated the dynamics, inducing "down" ("up") relaxation to lower (higher) Rydbergs.[15,26] Weak electric fields reduce the frequency of the close encounter of the Rydberg electron with the core, resulting in the retardation of the electronic-rotational energy exchange.[25,26] From the point of view of general methodology, the switching off of all the intramolecular decay channels implies new physical features, e.g., the breakdown of the Born–Oppenheimer separability for the relevant ultrahigh Rydbergs.[15–17,25,26] Such a picture seems to be incompatible with the general characteristics of low $l$ molecular Rydberg states, for which photoabsorption, electron-core interaction and intramolecular dynamics are manifested in the spatial region close to the nucleus (range $A$ in Fano's terminology[27,28]), where the potential and kinetic energies of the Rydberg election exceed the molecular vibrational and rotational energies. Accordingly, ultrahigh $n$ low $l$ states are expected to undergo "conventional" intramolecular relaxation in range $A$, and an "inverse" Born–Oppenheimer separation[15,25,26] is not warranted. Furthermore, in analogy to the theory of intramolecular dynamics,[1,29–32] the characterization of nonstationary ZEKE Rydbergs, which undergo rotational-induced relaxation (treated classically),[15,25,26] requires further elucidation. From the experimental point of view this model is applicable only for molecules and not for multichannel atoms, being apparently incompatible with the experimental observation (3). The further pursuit of this approach will be of interest.

(b) The $(l,m_l)$ Stark splitting and mixing model. Chupka proposed[21,22] that the Stark splitting and mixing of all the $l$ ZEKE Rydbergs (with a fixed $n$) is induced by very weak stray fields inevitably present in the system[33] or/and by the weak dc background electric field ($\sim0.1-1$ V/cm) in the experimental ZEKE setup.[15–20] This Stark mixing spreads the low $l$ ($=0-2$)

Rydberg wave function, which is active in absorption and intramolecular relaxation, among all the manifolds of the $n$ states. A ''democratic'' admixture of the active low $l$ state(s) results in an amplitude of $\sim n^{-1/2}$ in each eigenstate,[21,22,33,34] as originally proposed by Bordas *et al.*[34] in their study of electric field hindered vibrational autoionization. Accordingly, for the intramolecular decay channels $D(n) \propto n^{-1}$. Furthermore, Chupka[21,22] suggested that collisional interactions with neutrals and with ions could induce $m_l$ mixing, resulting in a manifold of $n^2$ states with $D(n) \propto n^{-2}$. Merkt and Zare[33] have modified Chupka's model[21,22] replacing the collisional $m_l$ mixing [which seems to be incompatible with observation (4)] by perturbations exerted by long-range electric fields of the static ions [in accord with observation (5)].

The Stark splitting and mixing model[21,22,33,34] considers the decay of a single eigenstate (or a small number of eigenstates), which is (are) optically selected from a dense manifold of eigenstates formed by $(l,m_l)$ mixing. This problem bears a close analogy to the intramolecular dynamics in isolated small[30–32,35] and large[30–32,36] molecules, where interstate mixing is induced by nonadiabatic or/and spin–orbit coupling,[1] while intrastate mixing is induced by anharmonic and Coriolis interactions.[37,38] In this paper we explore the consequences of the optical excitation process and the relation between the decay and the level structure within the dense mixed Stark manifold. We shall consider the dynamics of the dense mixed Stark manifold of high Rydbergs excited by a weak optical pulse, incorporating two new aspects, which pertain to the decay characteristics of the molecular eigenstates and excitation modes.

(a) The relation between the widths (reciprocal lifetimes) of the mixed eigenstates and the mean level spacing, which provides two limiting cases, i.e., the dense limit of overlapping resonances and the sparse limit of well-separated resonances. These limits bear a close analogy to the statistical limit and to the ''small molecule'' limit in intramolecular dynamics.[1,30–32,38]

(b) Optical excitation modes induced by a weak electromagnetic field of a variable temporal coherence length. The distinct response of the dense and sparse level structures will be considered.

The present note will attempt to elucidate the following interesting issues pertaining to the dynamics of the dense Stark manifold of many-electron atoms and of molecules.

(1) The determination of the domain of $n$ values where the lifetime of the doorway state can be determined.

(2) The determination of the range of $n$ values where isolated, nonoverlapping, mixed eigenstates can be optically excited. In this sparse domain the lengthening effect of the lifetime, i.e., the dilution of the lifetime of the doorway-exit state, will be exhibited.

(3) The identification of systems where the dense limit of mixed states can be realized over a narrow $n$ domain, where the lifetime is determined by the width of the distribution.

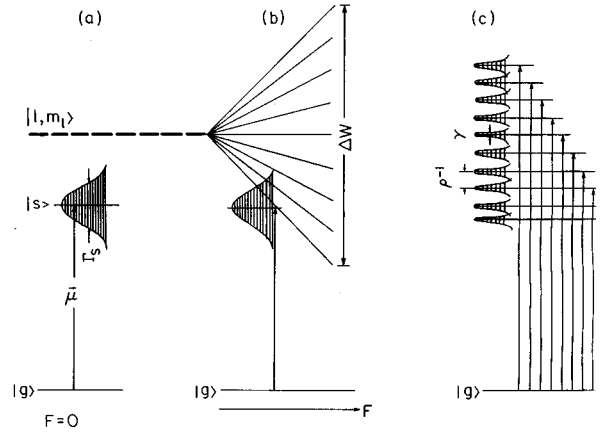


FIG. 1. A schematic energy level scene for the splitting and mixing of Rydberg states in an external electric field. (a) $F=0$. The low $l$ doorway state $|s\rangle$ is separated from the high $l$ degenerate manifold. The $|s\rangle$ state carries an oscillator strength from the ground state (denoted by a vertical arrow) and has a total nonradiative decay width $\Gamma_s$, which constitutes a sum of the partial decay widths of all, e.g., internal conversion, predissociation, and/or autoionization, channels. (b) The $F$ dependence of the splitting of the high $l$ manifold in the external field, which results in the onset of the merging of the $|s\rangle$ state into the manifold. (c) Mixed independently decaying levels at a finite field, which are characterized by coarse grained widths $\gamma \simeq \Gamma_s D(n)$ and density of states $\rho$. All these levels carry oscillator strengths from the ground state.

(4) The characterization of the response of the dense and sparse level structures to the optical excitation mode. The interrogation of the total population probability of the Rydberg manifold will result in a superposition of exponential temporal decay terms. In the exploration of the population probability of the doorway state wave packet dynamics internal dephasing and quantum beat phenomena[37] will be exhibited in the sparse limit, while the decay of a giant resonance[26,28] will be manifested in the dense limit.

## III. RYDBERG LEVEL STRUCTURE

A Rydberg state of a molecule or multichannel atom interrogated by ZEKE spectroscopy corresponds to $n$ in the range ~80–250. For a single $n$ in a zero electric field, the doorway state(s)[1,26,28] for optical excitation from the ground state and the escape state(s)[26,28] for intramolecular radiationless decay (predissociation, internal conversion, vibrational autoionization) correspond to a small number of $l,m_l$ states with low value(s) of $l$ (0–2). For the sake of simplicity we shall represent the doorway state(s) $|s\rangle$ by a single state [characterized by a low value(s) of $l=l_s$ and $m=m_s$] with the energy $E_s = \mathrm{IP} - R/(n-\delta)^2$ and the total nonradiative decay width $\Gamma_s \equiv \Gamma(n)$, Eqs. (1.1) and (1.2), i.e., $\Gamma_s = \Gamma_0/n^3$. At zero field this state is separated from the degenerate hydrogenic manifold of $(n^2-1)$ high $l,m_l$ states $(l>l_s)$ with the energies $E_l = \mathrm{IP} - R/n^2$ and decay widths $\Gamma_l = 0$, which are not optically accessible from the ground state (Fig. 1). In the presence of a weak ($F \sim 1$ V/cm) homogeneous electric field $F$, and of the inhomogeneous electric field exerted by the ions,[33] the effective Hamiltonian[31,32,39] for the system is

$$\mathbf{H}_{\mathrm{eff}} = \mathbf{H}_0 - (i/2)\boldsymbol{\Gamma} + \mathbf{H}_{\mathrm{STARK}} + \mathbf{V}, \tag{3.1}$$

TABLE I. Characterization of mixing and level structure of high molecular and atomic Rydbergs.

| Rydberg system | Decay channels | $\Gamma_0$ ($cm^{-1}$) | $\delta$ | $n_1$[c] | $\gamma\rho$[d] |
|---|---|---|---|---|---|
| DABCO $n=11-53$[a] | Vibrational autoionization internal conversion predissociation | $3.0\times10^3$ | 0.41 | 67 | $1.8\times10^{-2}$ |
| BBC $n=12-35$[a] | internal conversion | $10^3$ | 1.38 | 66 | $6\times10^{-3}$ |
| Xe[b] $d$ series | autoionization | $3.2\times10^4$ | 2.32 | 64 | 0.23 |
| Xe[b] $s$ series | autoionization | $10^3$ | 4.00 | | $0.7\times10^{-3}$ |
| Ar[b] $d$ series | autoionization | $4.0\times10^4$ | 0.26 | 61 | 0.39 |
| Ar[b] $s$ series | autoionization | $2.3\times10^3$ | 2.14 | 54 | $3.7\times10^{-2}$ |
| Ne[b] $d$ series | autoionization | $1.4\times10^4$ | 0.015 | 35 | 2.4 |
| Ne[b] $s$ series | autoionization | $3.7\times10^2$ | 1.30 | 63 | $2.8\times10^{-3}$ |

[a]Reference 15.
[b]References 41 and 42.
[c]$n_1=n_M F^{1/5}$, Eq. (3.4).
[d]$\gamma\rho$ at $n=n_M$, Eq. (3.9).

where $\mathbf{H}_0$ is the (diagonal) field-free Hamiltonian with the energies $E_s$ and $\{E_l\}$. $\mathbf{\Gamma}$ is the diagonal decay matrix with the elements $\Gamma_s$, $\{\Gamma_l=0\}$. $\mathbf{H}_{\mathrm{STARK}}$ is the Stark Hamiltonian with the operator $eFz$ coupling the doorway state $l_s m_s$ and the states $\{l',m'\}$ with $l'=l_s+1$, $m'=m_s$, while the states $\{l,m_l\}$ are coupled with $\{l'=l\pm1,\ m_l\}$. $\mathbf{V}$ is the off-diagonal perturbation exerted by the static ions.[33] The $n^2 x n^2$ effective Hamiltonian Eq. (3.1) can be diagonalized by a complex orthogonal transformation, resulting in the independently decaying levels[31,32,39] of the system

$$|j\rangle=a_s^{(j)}|s\rangle+\sum_l\sum_{m_l} b_{l,m_l}^{(j)}|l,m_l\rangle, \tag{3.2}$$

where $a_s^{(j)}$ and $\{b_{l,m_l}^{(j)}\}$ are (complex) coefficients. The (complex) eigenvalues are $[E_j-(i/2)\gamma_j]$, where $E_j$ are the energy levels and $\gamma_j$ the decay rates of the molecular eigenstates. (From now on we shall set $\hbar=1$ in all our equations.) In what follows we shall consider some limiting situations of the decaying level structure.

(1) The "isolated" doorway state (Fig. 1). The $E_s$ resonance at $F=0$ is well separated in energy from the $E_l$ manifold (Fig. 1). When the very weak electric field is increased, the $|s\rangle$ state will undergo a quadratic Stark shift, while the $\{|l,m_l\rangle\}$ manifold will undergo a linear Stark mixing and splitting.[40] The physical situation of an "isolated" $|s\rangle$ will be realized when the zero-field splitting $|E_s-E_l|\simeq 2\delta R/n^3$ [with $\delta=\delta(\mathrm{mod}1)$] exceeds $\Delta W/2$, where $\Delta W$ is the energetic spread of the Stark manifold of the $(n^2-1)$ $|l,m_l\rangle$ states

$$\Delta W=6Rn^2(F/5.14\times10^9), \tag{3.3}$$

(where $F$ is expressed in V $cm^{-1}$). Accordingly, when $F<3.4\times10^9\delta/n^5$ the mixing of $|s\rangle$ with the $\{|l,m_l\rangle\}$ manifold is weak and the doorway state retains its identity. Under these conditions (see Fig. 1) the resonance width $\Gamma_s$ of the isolated doorway state can be interrogated by optical spectroscopy. The experimental spectroscopic studies of Even *et al.*[15] on the vibrationally autoionizing Rydberg states of DABCO ($\delta=0.4$), which were conducted in weak electric fields ($F\leqslant1$ V/cm), allow for studies of the linewidth $\Gamma_s$ for $n<67$. In fact, isolated Rydberg resonances were observed by Even *et al.*[15] up to $n\simeq52$. However, this upper limit for the observation of the isolated low $l$ Rydbergs is not intrinsic, being limited by the experimental conditions.

(2) The strong mixing of the doorway state with the $\{|l,m_l\rangle\}$ manifold. This situation will be realized when the energetic spread $\Delta W/2$ exceeds the zero-field splitting $2\delta R/n^3$. When $|E_s-E_l|<\Delta W/2$ (Fig. 1), the doorway state strongly mixes with the hydrogenic higher $l$ manifold. This situation will be realized when

$$F>3.4\times10^9\delta/n^5. \tag{3.4}$$

Condition (3.4) for effective mixing is expected to be applicable for the Rydberg manifold of molecules and of many-electron atoms. The lower limit $n_M$ for the $n$ values for strong mixing is specified by $n_M=n_1(F/\mathrm{V\ cm^{-1}})^{-1/5}$ where $n_1=80.5\,\delta^{1/5}$. In Table I we present the $n_1$ data for the Rydberg manifolds of the DABCO and BBC molecules[15] as well as for the autoionizing $s$ and $d$ series of the rare-gas atoms.[41,42]

In the domain $n\geqslant n_M$ the energetics and dynamics of the system will be dominated by the strong mixing of the doorway state among the split and mixed $(l,m_l)$ levels. The diagonalization of the effective Hamiltonian, Eq. (3.1), will result in $J$ molecular states in the energy domain $\Delta W$, being characterized by the individual decay widths $\gamma_j$. The width

$\Gamma_s$ of the doorway state is then diluted among the molecular eigenstates. The dilution factor $D(n)$ will be approximated by a coarse grained quantity with an equal contribution to all the eigenstates, i.e., $D(n)=1/J$, so that the decay widths of the individual molecular eigenstates $\gamma \simeq \gamma_j$ (all $j$) will be given by

$$\gamma \approx \Gamma_s D(n). \tag{3.5}$$

These averaged decay widths are determined by the nature of the dilution. In the absence of perturbing ions ($\mathbf{V}=0$), a homogeneous field results in Stark ($l$) splitting, so that $D(n) \simeq 1/n$ and $\gamma \simeq \Gamma_s/n$. In the case of $(l,m_l)$ mixing, $D(n) \simeq 1/n^2$ and $\gamma \simeq \Gamma_s/n^2$.

The averaged energetic spacing between the adjacent molecular eigenstates is

$$\rho^{-1}=\Delta W/J, \tag{3.6}$$

being characterized by the density of states $\rho$. We can now distinguish between the situations of the dense limit of overlapping resonances

$$\gamma\rho > 1 \tag{3.7a}$$

and of the sparse limit of separated resonances

$$\gamma\rho \ll 1. \tag{3.7b}$$

From Eqs. (3.5) and (3.6) we infer that $\gamma\rho=\Gamma_s/\Delta W$, whereupon the dense limit can be realized when $\Gamma_s/\Delta W>1$, while the sparse limit prevails when $\Gamma_s/\Delta W \ll 1$. We note that these conditions are independent of $D(n)$. Equations (1.1) and (3.3) result in

$$\Gamma_s/\Delta W = 0.86\times 10^9 \Gamma_0/RFn^5. \tag{3.8}$$

The magnitude of the parameter $\Gamma_s/\Delta W$, in conjunction with the merging condition, determines the level structure. At the onset of merging, i.e., for $n=n_M$, Eq. (3.8) results in

$$\gamma\rho=\Gamma_0/4\delta R; \quad n=n_M. \tag{3.9}$$

We note that $\gamma\rho$ at $n=n_M$ is independent of $n_M$ and of the external field strength. For $n>n_M$ we have

$$\gamma\rho=(\Gamma_0/4\delta R)(n_M/n)^5; \quad n>n_M, \tag{3.10}$$

which decreases as $n^{-5}$ and is proportional to $F$. From this analysis we conclude that

(a) $n_M$, which provides the signature of the onset of strong level mixing, is independent of $D(n)$, being essentially identical for both ($l$) and for $(l,m_l)$ mixing.

(b) The parameter $\gamma\rho$ at $n=n_M$, which determines the level structure of the mixed states, is determined by the ratio $\Gamma_0/4\delta R$, being independent of $n_M$.

(c) The parameter $\gamma\rho$ at $n>n_M$ decreases as $n^{-5}$ with increasing $n$.

(d) The parameters $n_M$ and $\gamma\rho$ are independent of $D(n)$, being invariant with respect to the mixing mechanism, i.e., being identical for ($l$) mixing and for $(l,m_l)$ mixing. The partial width $\gamma$, Eq. (3.5), is, of course, determined by the mixing mechanism.

(e) The energetic spread $\Delta W$, Eq. (3.3), of the mixed states is essentially unrelated to the intrinsic resonance width $\Gamma_s$.

(f) Regarding the external electric field dependence of the relevant parameters, we note that $n_M \propto F^{-1/5}$ and $\Delta W \propto F$, $\gamma\rho(n=n_M)$ is independent of $F$, while $\gamma\rho(n>n_M) \propto F^{-1}$.

(g) In the vicinity of $n \gtrsim n_M$ the level structure can correspond either to the dense limit [case (a)] or to the sparse limit [case (b)]. For $n \gg n_M$ the level structure always corresponds to the sparse limit.

(h) The interrogation of the mixed Rydberg level structure (in the domain $n \gtrsim n_M$) by time-resolved or energy-resolved experiments will not result in the total resonance width $\Gamma_s$. Rather, the relevant energetic (i.e., lifetime) parameters which emerge from the analysis of the total population of the Rydberg manifold correspond to $\gamma$. The exploration of the population of the doorway state will result in $\gamma$ for the sparse limit or in $\Delta W$ (and $\Gamma_s$) for the dense limit (Sec. IV).

From the foregoing general analysis we infer that the level structure of strongly mixed atomic and molecular high ZEKE Rydbergs can correspond to the following two limiting situations:

(a) A dense limit for $n=n_M$ changing to the sparse limit for $n \gg n_M$. This physical situation is realized when $\Gamma_0/4\delta R>1$.

(b) A sparse limit for all $n(\geq n_M)$, i.e., $\Gamma_0/4\delta R<1$.

From the values of $\gamma\rho$ (at $n=n_M$) estimated for the molecular Rydberg series of DABCO and BBC,[15] and for the autoionization of $s$ and $d$ Rydbergs of some rare-gas atoms (Table I) we infer that

(1) The Rydbergs of the DABCO and BBC correspond to the sparse limit of isolated resonances for all relevant $n$ [case (b)].

(2) The mixing of the $s$ Rydbergs of rare-gas atoms are characterized by low values of $\Gamma_0$.[41,42]

(3) The mixing of the $d$ Rydbergs of Ar or of Ne, which are characterized by high values of $\Gamma_0$ and by low values of $\delta$, are characterized by high values of $\gamma\rho$. Then Rydbergs of $n \gtrsim n_M$ exhibit overlapping resonances.

(4) The mixing of the $d$ Rydbergs of Ar and Xe correspond to an intermediate situation between cases (a) and (b).

(5) Of considerable interest is the mixing of the $d$ Rydbergs of Ne, which corresponds to case (a). For a typical field of $F=1$ V/cm, we expect the dense limit to prevail from $n=n_1=35$ (Table I), up to $n \simeq 50$, while the sparse limit sets in for $n>70$.

(6) Both the sparse and the dense mixed Rydberg level structures can be realized under realistic physical conditions.

## IV. LIFETIMES AND DECAY MODES OF A STRONGLY MIXED RYDBERG MANIFOLD

We are concerned with the optical excitation to and the decay of a congested level structure of a single high $n(\geq n_M)$ Rydberg manifold subjected to $(l,m_l)$ or to ($l$) mixing, a

problem which is analogous to the theory of time-resolved photon scattering from excited molecular states.[30–32] The issues we would like to address are

(1) Under what conditions will the diluted lifetime, Eq. (1.5), be exhibited?
(2) What are the observable decay modes for distinct (dense or sparse) level structures under different optical excitation conditions?

The strongly mixed and split Rydberg manifold will be excited by a weak electromagnetic light pulse which is characterized by an electromagnetic field $\epsilon(t) = \epsilon_0 \exp(i\bar{E}t) \exp(-|t|/\tau_p)$, and the autocorrelation function is $\langle \epsilon^*(t)\epsilon(0)\rangle = \langle|\epsilon(0)|^2\rangle \exp(i\bar{E}t) \exp(-\Delta\omega_p t/2)$, where $\epsilon_0$ is the pulse amplitude, $E$ is the central energy, $\tau_p$ the pulse decay time, and $\Delta\omega_p$ corresponds to the spectral width of the light pulse. For a conventional ns dye laser commonly used in ZEKE experiments[15–24] $1/\tau_p = 5\times10^{-3}$ $cm^{-1}$, and the laser pulse is not uncertainty limited with phase and energy laser fluctuations spanning the energy range $\Delta\omega_p = 0.1-0.5$ $cm^{-1}$. For ps and fs lasers $\Delta\omega_p \simeq 1-500$ $cm^{-1}$, the laser pulse being uncertainty limited with $1/\tau_p \simeq \Delta\omega_p$. Now, the $|s\rangle$ state constitutes the doorway state for optical excitation from the ground state $|g\rangle$ and the time evolution of the system is monitored.

To make contact with the experimental real-life situation, we consider two experimental observables (Appendix).

(a) The excited-state total population probability $P(t)$. This corresponds to the time-dependent population of the entire Rydberg manifold. $P(t)$ is interrogated by time-resolved ZEKE spectroscopy,[15–20] by the application of the extracting pulsed electric field at the delay time $t$ after the optical laser field.
(b) The population probability $I(t)$ of the doorway state $|s\rangle$. $I(t)$ represents the time-dependent population of the low angular momentum state(s) $|s\rangle$, which is (are) active in absorption. In principle, $I(t)$ could be monitored by time-resolved fluorescence[30–32] to the ground state, however, the extremely low oscillator strengths (and extremely long radiative lifetimes, i.e., $\propto n^3$) of high Rydbergs preclude this approach. $I(t)$ can be experimentally interrogated by the subsequent photoionization of the Rydberg manifold, with the doorway state being also the active state for ionization. In this Rydberg photoionization experiment a second ionizing light pulse should be applied at the delay time $t$ after the exciting optical laser pulse.

The excited-state population probability $P(t)$ is interrogated by the novel method of time-resolved ZEKE spectroscopy.[15–18,19(e),19(f)] The excited-state population probability (apart from proportionality constraints) is obtained (see Appendix) from Eqs. (A4), (A8), and (A9) in the form

$$P(t) = \sum_j |a_j^{(s)}|^2 \int_{-\infty}^{t} d\tau \int_{-\infty}^{t} d\tau' f_j^*(t-\tau') f_j(t-\tau) \otimes \langle \epsilon^*(\tau')\epsilon(\tau)\rangle, \tag{4.1}$$

where the coefficients $a_j^{(s)}$ are given from Eq. (3.2), the functions $f_j(x)$ are given by Eq. (A9), while $E_j$ and $\gamma_j$ are the energies and decay widths of the molecular eigenstates, respectively. Let us consider first $P(t)$ for a sparse level structure, i.e., $\gamma_j \ll |E_j - E_{j'}|$ for all $j$ and $j'$. Under these circumstances the photoselection of a single molecular state $j$ can be realized when

$$|E_j - E_{j\pm1}| \gg \Delta\omega_p \gg \gamma_j. \tag{4.2}$$

The decay will be then of the approximate form $P(t) \propto \exp(-\gamma_j t)$. Next, we consider the excitation of several molecular eigenstates when $\Delta W > \Delta\omega_p \gg \gamma_j$. Under these circumstances a wave packet of several eigenstates is initially excited. The total population probability consists of several decay terms

$$P(t) = \sum_j |B_j|^2 \exp(-\gamma_j t), \tag{4.3}$$

where

$$B_j = a_s^{(j)}/[E_j - \bar{E} - (i/2)\Delta\omega_p]. \tag{4.4}$$

$P(t)$ in Eq. (4.3) corresponds to the sum of decaying exponentials, with lifetimes $\gamma_j$, while the amplitudes $|B_j|^2$ are determined by the excitation coefficients $|a_s^{(j)}|^2$ weighted by the Lorentzian line shape of the excitation pulse. Finally, we consider the broad-band excitation when $\Delta\omega_p \gg \Delta W$, and the entire sparse manifold is excited by the ''white'' light pulse, which in this case is $\langle \epsilon(0)\epsilon(t)\rangle = \delta(t)$. The population probability is then

$$P(t) = \sum_j |a_s^{(j)}|^2 \exp(-\gamma_j t), \tag{4.5}$$

exhibiting a superposition of decaying exponentials for all times $t$. Next, we turn to $P(t)$ for the dense level structure, i.e., $\gamma_j > |E_j - E_{j\pm1}|$ for all $j$. This limit corresponds to case (a) for $n \geqslant n_M$. For overlapping resonances, the excitation of a single eigenstate cannot be accomplished.[1,30–32] A wave packet of overlapping eigenstates can be excited. When $\Delta W > \Delta\omega_p \gg \gamma_j$, a wave packet of several overlapping resonances is excited. The total population probability for the dense limit is given by Eqs. (4.3) and (4.4). For the broad-band excitation of the dense level structure, i.e., $\Delta\omega_p \gg W$, $P(t)$ is given by Eq. (4.5).

From this analysis of the population probabilities three conclusions emerge. First, the only difference between the sparse and dense level structures is that the photoselection of a single molecular eigenstate is possible only in the sparse limit. Second, the total population probabilities for the dynamics of partial or of coherent wave packets are identical for the sparse and the dense limits. Thus both in the sparse limit (for $\Delta\omega_p > |E_j - E_{j'}|$), and in the dense limit, $P(t)$ is obtained in terms of a superposition of decaying exponentials. Third, the time-dependence of the excited state population probability for both the sparse and the dense level structures and under all excitation conditions, contains only a superposition of exponential decay terms and does not contain interference terms, i.e., temporal quantum beats. As is known from the theory of intramolecular dynamics,[30–32,39] the total decay probability involves only direct exponential

decay terms, while quantum beats can be manifested by decay of a specific wave packet of states (i.e., a subspace of the discrete Hilbert space), such as the decay of the doorway state.

As all the available experimental information on the dynamics of high Rydbergs emerges from time-resolved ZEKE experiments,[15–20] the characterization of the feasible experimental conditions is of interest. Taking $(\Delta W/\mathrm{cm}^{-1})=1.3\times10^{-4}n_M^2$ $(F/\mathrm{V\ cm}^{-1})$ at $n=n_M$, we estimate (for $F=0.1$ $\mathrm{V\ cm}^{-1}$) that $\Delta W=0.13$ $\mathrm{cm}^{-1}$ for $n_M=100$ and that $\Delta W=0.033$ $\mathrm{cm}^{-1}$ for $n_M=50$. We infer that for a conventional ns laser $(\Delta\omega_p\simeq0.1-0.5$ $\mathrm{cm}^{-1})$ $\Delta\omega_p>\Delta W$, so that broad-band excitation will be accomplished under ns excitation. The population decay pattern is expected to be given by Eq. (4.6). On the basis of general coarse graining arguments we expect that for strong mixing the averaged reciprocal lifetimes will be $\langle\gamma_j\rangle\simeq\Gamma_s D(n)$ with $D(n)$ being in the range $1/n$ (for $l$ mixing) to $1/n^2$ (for $lm_l$ mixing). Of course, the decay will not be strictly exponential and will involve a superposition of exponentials, reflecting some homogeneous distribution of the decay times.

Complementary information on the decay dynamics and coherence effects will emerge from the population probability $I(t)$ of the doorway state $|s\rangle$. The interrogation of $I(t)$ by photoionization of the Rydberg manifold for high $(n\simeq80-250)$ states constitutes an experimental challenge, which was not yet undertaken. Such an approach was already utilized to probe temporal coherence, i.e., quantum beats in the time evolution of a wave packet of bound atomic Rydbergs.[43,44] Accordingly, the exploration of $I(t)$ is of interest. Equations (A6), (A8), and (A9) result in the explicit expression

$$I(t)=\sum_j\sum_{j'}|a_s^{(j)}|^2|a_s^{(j')}|^2\int_{-\infty}^{t}d\tau\int_{-\infty}^{t}d\tau' f_j(t-\tau)\times f_{j'}^{*}(t-\tau')\langle\epsilon^{*}(\tau')\epsilon(\tau)\rangle, \tag{4.6}$$

where the coefficients $a_s^{(j)}$ are given by Eq. (3.2), and $f_j(x)$ is defined by Eq. (A9). As is well known,[30–32] $I(t)$ contains a direct term $(j=j')$ and oscillatory terms $(j\neq j')$.

Consider $I(t)$ for a sparse level structure. The photoselection of a single molecular eigenstate will be realized under condition (4.2). The decay will be of the approximate form $I(t)\propto\exp(-\gamma_j t)$, being of the same form as $P(t)$ for this physical situation. More interesting is the excitation of several molecular eigenstates. Equation (4.6) consists now of several direct terms and of oscillatory interference terms

$$I(t)=\sum_j|B_j|^2\exp(-\gamma_j t)+\sum_j\sum_{j'}B_j^{*}B_j\times\exp[i(E_{j'}-E_j)t]\exp[-(\gamma_j+\gamma_{j'})t/2], \tag{4.7}$$

where $B_j$ is given by Eq. (4.4). The single sum in Eq. (4.7) corresponds to a sum of decaying exponentials, as for $P(t)$, Eq. (4.3). The interference term manifests temporal oscillations with frequencies $\hbar/(E_j-E_{j'})$ of the optically accessible states. Finally, we consider broad band excitation of the sparse manifold, i.e., $\Delta\omega_p\gg\Delta W$. The doorway state population probability is

$$I(t)=\sum_j\sum_{j'}|a_S^{(j)}|^2|a_S^{(j')}|^2\times\exp\left[-\left(\frac{\gamma_j+\gamma_{j'}}{2}\right)t+i(E_{j'}-E_j)t\right]. \tag{4.8}$$

For the short time domain $(\Delta\omega_p)^{-1}<t$ and $t\lesssim(\Delta W/J)^{-1}\ll\gamma_j^{-1}$, which corresponds to the recurrence relation,[1] the decay mode being $I_s(t)=\exp(-t\Delta W)$. For long times $t\gg(\Delta W/J)^{-1}$, exceeding the recurrence time, the interference terms in Eq. (4.4) vanish and the molecular eigenstates will exhibit an independent decay of the form $I_L(t)\simeq\Sigma_j|a_j^{(s)}|^4\exp(-\gamma_j t)$, corresponding to a superposition of decaying exponentials, analogous to $P(t)$, Eq. (4.5). The ratio between the amplitude of the decay modes of the coherent component and of the long component is $I_s(0)/I_L(0)\simeq1/J$. Thus the interrogation of $I_s(t)$ for the total manifold is of minor physical interest. What will be of considerable interest is the conduction of photon echo or FID decay experiments to monitor the coherence decay of the manifold.[37,38]

Of considerable interest in the population probability of the doorway state is the second limit of the dense level structure, i.e., $\gamma_j>|E_j-E_{j\pm1}|$ for all $j$. This limit corresponds to case (a) for $n\gtrsim n_M$. For overlapping resonances, the excitation of a single molecular eigenstate cannot be accomplished.[1,30–32] This physical situation for $I(t)$ is analogous to photon scattering from a giant resonance[32] of width $\Delta W$ (with $\Delta W\gg\Gamma_s$) and a central energy $E_0$ with the population probability being of the form[30–32]

$$I(t)\propto\exp(-t\Delta W)+\exp(-t\Delta\omega_p)+\exp[i(E_0-\bar{E})t]\times\exp\left[-\left(\frac{\Delta W+\Delta\omega_p}{2}\right)t\right]. \tag{4.9}$$

The time evolution, Eq. (4.9), consists of a ''molecular'' decay characterized by a decay time $\sim\hbar(\Delta W)^{-1}$ of the pulse decay and an interference term. The only ''molecular'' lifetime corresponds to $\hbar(\Delta W)^{-1}$, which can be also explored by ps or fs excitation in conjunction with the interrogation of coherent optical effects, e.g., photon echoes or free-induction decay.[37,38] A possible victim for the exploration of this novel domain for $I(t)$ may involve the mixing of the autoionizing $d$ series of Ne. From this analysis we conclude that the interrogation of $I(t)$ will provide a distinction between the sparse and the dense level structure of high Rydbergs.

## V. CONCLUDING REMARKS

Our analysis of the novel features[15–24] of the dynamics of extremely high Rydbergs pursues a formal analogy between relaxation phenomena in a bound level structure originating from intramolecular (interstate and intrastate) coupling and from the mixing of the $l$ components of a high Rydberg in external electric field(s). The basic physical picture of coupling and dynamics in a bound level structure

formally rests on the partition of the Hilbert space into the relevant discrete level structure and the continuum (or quasicontinuum) decay channels, together with the characterization of the accessibility conditions (via excitation) of the former subspace. It is also applicable for the description of the dynamics of the ZEKE Rydbergs, which is characterized by the following features: (a) The relevant discrete level structure consists of a low $l$ state(s) and a hydrogenic manifold of high $l$. (b) The few low $l$ state(s) constitute the doorway state(s) for excitation. (c) The low $l$ state(s) are coupled to decay channels, i.e., internal conversion, predissociation and/or vibrational autoionization for molecular Rydbergs and atomic spin–orbit autoionization for atomic Rydbergs. (d) The discrete subspace is mixed via ($\mathbf{H}_{\mathrm{STARK}}+\mathbf{V}$) in Eq. (3.1). The nature of the coupling and structure of the effective Hamiltonian differs, of course, for intramolecular coupling and for the electric field induced high-Rydberg mixing. While the (imaginary) decay contribution $-i\Gamma_s/2$ to $\mathbf{H}_{\mathrm{eff}}$, Eq. (3.1), is identical for both cases, the nature and details of the couplings are qualitatively different. For intramolecular (interstate and intrastate) coupling the doorway state couples in parallel to the entire background manifold and the individual relevant coupling terms are of comparable magnitude.[29–32,35] On the other hand, the electric field induced coupling between the zero-order Rydbergs, due to $\mathbf{H}_{\mathrm{STARK}}$ in Eq. (3.1), is[40] (i) sequential, with $l-(l\pm1)$ nonvanishing matrix elements, and (ii) hierarchial, with the sequential matrix elements decreasing with increasing $l$, being proportional to $n^2$ for low $l$ and being proportional to $n$ for high $l$. This qualitative difference between intramolecular and Stark coupling also results in a difference in the mixed level structure. For intramolecular coupling the doorway state is usually located within the energy domain of the background manifold and mixed with it.[29–32,35] On the other hand, when field induced mixing of Rydbergs with increasing $F$ is accomplished at a constant $n$, the doorway state does not energetically overlap the Stark split inactive manifold, but rather approaches it from its low energy range. This problem is analogous to the coupling of a discrete zero-order state with a manifold, which is bound from below.[45] Strong mixing is then accomplished when condition (3.4) is fulfilled. This physical situation of the doorway state ''approaching the manifold from below'' is clearly demonstrated for the energetics in the atlas maps of the Stark levels[46] of the $n=15$ atomic Rydbergs of alkali atoms, e.g., Figs. 6–8 of Ref. 46. These Stark spectra[46] beautifully demonstrate the mixing of the doorway state, with the onset of strong mixing of the $15p$ ($m=0$) doorway state [with $\delta=0.05$ (Ref. 45)] into the $n=15$ manifold being realized at $F>250$ V/cm, with this value of $F$ being in accord with Eq. (3.4). This transparent physical situation is realized for a low quantum defect ($\delta\ll0.5$), when the mixing between neighboring different $n$ manifolds is negligible. Of course, the bound alkali Rydberg spectra[46] pertain solely to the energetics and the oscillator strength of the mixed level structure and do not provide any dynamic information, which is the central theme of the present study.

When field-induced Rydberg strong mixing has been accomplished, the gross physical features of intramolecular dynamics and the dynamics of the (strongly mixed) Rydberg level structure bear a close analogy. In particular, our distinction between the sparse and dense level structures for the energetics and dynamics of high Rydbergs is analogous to the small molecule limit and the statistical limit, respectively, for intramolecular dynamics.[30–32,35,36] From the experimental point of view all the information currently available on the decay dynamics of molecular[15–18,19(e),19(f),21,22] and atomic[24] ZEKE Rydbergs in weak ($F\sim0.1-5$ V cm$^{-1}$) external fields corresponds to the sparse limit.

Our analysis of the novel features of the level structure and dynamics of high Rydbergs focused on the strong mixing situation, with $F$ being determined by condition (3.4), i.e., $F>3.4\times10^9\delta/n^3$. Our treatment has been limited to a mixing with a single $n$ manifold, which is realized for $\Delta W/2<R/n^3$, i.e., $F<1.7\times10^9/n^5$. When the latter condition is violated, mixing of several $n$ manifolds will occur. However, this effect will not modify the gross features of the level structure and dynamics for strong mixing. In this situation we were able to

(1) Characterize the dilution effect of the doorway state on the lifetimes of the strongly mixed Rydberg manifold, with the coarse grained average decay rate being $\langle\gamma\rangle\simeq\Gamma_s D(n)$ [$D(n)\ll1$, being $\sim n^{-1}$ for ($l$) mixing and $\sim n^{-2}$ for ($lm_l$) mixing], in accord with the interpretation originally proposed by Bordas *et al.*[34] by Chupka,[21,22] and by Merkt and Zare.[33] What is new in our analysis is the advancement of the theoretical framework for a detailed calculation of the level structure (Sec. III) and the dynamics (Secs. III and IV). Making contact with real-life situations, we note the experimental data for the DABCO and BBC high Rydbergs,[15] which exhibit long ZEKE lifetimes for $n>100$ for BBC and $n>63$ for DABCO, where for $n\simeq100$, $D(n)\sim10^{-2}$ for BBC and $D(n)\simeq3\times10^{-3}$ for DABCO. These experimental results are consistent with the $n_1$ data presented in Table I and with the rough estimate of $D(n)$ for ($l$) mixing. Accordingly, under the experimental conditions of ZEKE spectroscopy with a dc field in the range $F\simeq1$ V cm$^{-1}$, which was employed by Even *et al.*,[15] the strong ($l$) mixing situation is realized.
(2) Provide a new and useful classification of the strongly mixed Rydberg level structure in terms of the distinct sparse and dense level structures.
(3) Specify the decay modes of the total population decay $P(t)$ and of the decay of the doorway state $I(t)$. $P(t)$ is expected to involve a superposition of exponentials for both the sparse and dense level structures and for all excitation modes. The interrogation of $I(t)$ will result in the possibility of the observation of quantum beats in the decay of a few molecular eigenstates in the sparse limit and the observation of a giant resonance in the dense limit.
(4) Assert a ''universality'' principle for the unified description of the level structure and dynamics of high Rydbergs of molecules and of autoionizing atoms.

The strong mixing situation constitutes an important limiting case for the understanding of the level structure and the

dynamics of high Rydbergs. This strong mixing limit does not set up abruptly. Rather, we expect that a gradual enhancement of the mixing of the doorway state $|s\rangle$ with the inactive $\{|l,m_l\rangle\}$ manifold will occur with increasing $F$. It will be useful to provide a qualitative description of the evolution of the field-induced mixing, limiting ourselves to the case of $(l)$ mixing. Taking a single doorway state as $|s\rangle=|l_s=0,\ m_l=0\rangle$ we have to consider sequential and hierarchial coupling to and within the inactive manifold $\{|l,m_l=0\rangle\}$. It will also be useful to specify the electric field, which induces the coupling, in terms of reduced units. Guided by Eq. (3.4) we scale the electric field in the useful form

$$\bar{F}=(F/\mathrm{V\ cm^{-1}})n^5/3.4\times10^9\delta. \tag{5.1}$$

For $\bar{F}=0$ the truly isolated $|s\rangle$ resonance is characterized by the lifetime $\tau_s=\hbar/\Gamma_s=\hbar n^3/\Gamma_0$. The level mixing at a finite $\bar{F}$ is characterized by the parameters $\delta$, $n$, and $\bar{F}$, which determine the mixing coefficients $a_s^{(j)}$ in Eq. (3.2), which are obtained from the diagonalization of $\mathbf{H}_{\mathrm{eff}}$ Eq. (3.1). With increasing $\bar{F}$ the doorway state $|s\rangle$ starts shifting and mixing towards the inactive $|l\rangle$ manifold, approaching it from below.[46] Thus for a single $n$ manifold, with $0<\delta(\mathrm{mod}1)\ll0.5$, the lowest energy eigenstate, which we denote by $|j=1\rangle$ in Eq. (3.2), with the mixing coefficient $a_s^{(1)}$, has a parentage in $|s\rangle$. For this $|j=1\rangle$ eigenstate $|a_s^{(1)}|^2\to1$ for $\bar{F}\to0$. The weight $|a_s^{(1)}|^2$ of the doorway state in the special $|j=1\rangle$ eigenstate will constitute an important parameter for the characterization of the decay dynamics.

For very low (reduced) electric fields, i.e., $\bar{F}<1$, weak mixing already sets in. Without alluding to detailed calculations, two distinct time scales are expected to be exhibited in this weak mixing regime.

(i) A short lifetime,

$$\tau_{\mathrm{SHORT}}\simeq\tau_s/|a_s^{(1)}|^2 \tag{5.2}$$

(where $\tau_s$ is on the ns time scale for an $n\sim100$ doorway Rydberg and so will be $\tau_{\mathrm{SHORT}}$). With increasing $\bar{F}(<1)$ $|a_s^{(1)}|^2$ decreases and we expect $\tau_{\mathrm{SHORT}}$ to increase (on the $\sim$1–10 ns time scale).

(ii) A broad distribution of long lifetimes. A very crude approximation provides an average value of

$$\langle\tau_{\mathrm{LONG}}\rangle\simeq n\tau_s/[1-|a_s^{(1)}|^2] \tag{5.3}$$

for these long lifetimes. In the weak mixing regime, we take for the sake of a rough estimate $|a_s^{(1)}|^2\simeq0.95-0.90$, resulting in $\langle\tau_{\mathrm{LONG}}\rangle\simeq(10-20)n\tau_s$, which for $n=100$ is in the $\mu$s time domain. With increasing $\bar{F}$, $\langle\tau_{\mathrm{LONG}}\rangle$ decreases, due to the decrease of $|a_s^{(1)}|^2$.

The total population probability in the weak mixing regime is approximately given by the superposition of the contributions from ranges (i) and (ii), in the form

$$P(t)\simeq|a_s^{(1)}|^2\ \exp(-t/\tau_{\mathrm{SHORT}})+[1-|a_s^{(1)}|^2]\times\ \exp(-t/\langle\tau_{\mathrm{LONG}}\rangle). \tag{5.4}$$

Although this relation does not do justice to the broad distribution of lifetimes in range (ii), it nicely demonstrates the separation of time scales in the weak mixing regime where $|a_s|^2\lesssim0.1$.

With the increase of $\bar{F}$ above $\bar{F}>1$ we expect that in range (i), $\tau_{\mathrm{SHORT}}$ increases (towards $n\tau_s$) and the amplitude $|a_s^{(1)}|^2$ of the short component decreases, while in range (ii) the average diluted value of $\langle\tau_{\mathrm{LONG}}\rangle$ tends towards $n\tau_s$. The strong mixing limit is realized for $\bar{F}>1$ with $|a_s^{(1)}|^2\to1/n$, $\tau_{\mathrm{SHORT}},\langle\tau_{\mathrm{LONG}}\rangle\to n\tau_s$. Then the contribution of range (i) to $P(t)$, Eq. (5.2), becomes small and indistinguishable from that of range (ii), which provides the dominating contribution to $P(t)$ with the mean lifetime $\tau_s/D(n)$. This heuristic, but physical, description predicts that

(1) Two distinct ($\sim$ns and $\sim\mu$s) time scales for the dynamics for $\bar{F}<1$ will be exhibited.
(2) The lengthening of the short (ns) temporal decay component with increasing $\bar{F}$ is expected for $\bar{F}<1$.
(3) A broad distribution of long lifetimes with the average value of $\simeq(10-20)n\tau_s$, i.e., in the $\mu$s time domain, is expected for $\bar{F}<1$.
(4) The long lifetimes exhibit a broad distribution.
(5) The average long lifetime decreases with increasing $\bar{F}$.
(6) Coalescence of the lifetimes towards the mean diluted lifetime $\tau_sD(n)$ occurs in the strong mixing limit $(\bar{F}>1)$, which constitutes the central theme of the present paper.

These predictions for the novel and rich dynamics in the weak mixing $(\bar{F}<1)$ domain provide guidelines for the understanding of experimental data. In particular, our analysis provides clues for

(a) The possibility of observation of extremely long ($\sim$ a few $\mu$s) lifetimes of ZEKE Rydbergs.[19(f)]
(b) Pronounced nonexponentiality of the long-time decay of ZEKE Rydbergs.[15,17,18,19(e),19(f)]
(c) The dramatic (two to three orders of magnitude) break in the Rydberg lifetimes vs $n$ (Ref. 15) which corresponds to the "transition" from range (i) to range (ii), occurs at $n\simeq n_M$ $(\bar{F}\sim1)$, when the contribution of range (ii) to the decay dynamics becomes dominant.

The central prediction for the occurrence of two distinct time scales for the dynamics of Rydbergs $(\bar{F}<1)$ was not yet verified experimentally. Our analysis calls for the extension of the time-resolved ZEKE technique into the time domain of 1–10 ns.

The picture of the "transition" from the weak mixing regime $(\bar{F}<1)$ to the strong mixing limit $(\bar{F}>1)$ has to be extended to include additional effects.

(1) Mixing of several $n$ manifolds. We have considered a single $n$ manifold, when the quantum defect is sufficiently low to preclude the mixing of several $n$ manifolds, i.e., $\bar{F}<1/2\delta$. For larger values of $\delta$ ($\sim$0.3–0.5), the mixing of several doorway states and of several $n$ manifolds will be significant and the physical picture for the level structure and dynamics in the strong mixing limit will be qualitatively modified.

(2) Multichannel mixing. Our simple picture, which rests on a single doorway state and a single escape (decaying) state, has to be modified. Several low $l$ states ($l=0-3$), each characterized by a distinct quantum defect and decay width, have to be incorporated in the effective Hamiltonian, Eq. (3.1). In some cases the decay matrix in $i\mathbf{\Gamma}/2$ is nondiagonal. The doorway state(s) are determined by the specific, e.g., one-photon or two-photon excitation conditions.

Our physical picture for the level structure and dynamics of high Rydbergs considered herein is truly full of surprises, providing an exciting hunting ground for further experimental and theoretical studies.

## ACKNOWLEDGMENTS

We are grateful to Professor Uzi Even, Professor Richard Bersohn, Professor Raphael D. Levine, Professor Ed Grant, Professor Edward W. Schlag, and Professor Richard N. Zare for stimulating discussions and for their incisive comments on this manuscript. We are grateful to Professor Richard N. Zare for prepublication information. This research was supported by the Binational German–Israeli James Franck Program on Laser–Matter Interactions.

## APPENDIX: THE TIME DEPENDENCE OF THE POPULATION OF THE RYDBERG MANIFOLD

The molecular or atomic system is characterized by the ground state $|g\rangle$ with the energy $E_g=0$ and the molecular eigenstates $|j\rangle$, Eq. (3.2), with the complex energies $E_j-(i/2)\gamma_j$. The system is driven by a (weak) electromagnetic field $\epsilon(t)$, whose autocorrelation function is

$$\langle \epsilon^*(t)\epsilon(0)\rangle = \exp(i\bar{E}t)\exp(-\Delta\omega_p t/2), \tag{A1}$$

where $\Delta\omega_p$ is the spectral width of the light pulse and $\bar{E}$ is the central energy of the pulse. The time dependent wave function is given in the interaction representation

$$\bar{\Psi}(t) = C_g(t)|g\rangle + \sum_j C_j(t)\ \exp(-iE_j t)|j\rangle, \tag{A2}$$

with the time dependent amplitudes $C_g(t)$ and $\{C_j(t)\}$ obeying the initial conditions $C_g(-\infty)=1$, and $C_j(-\infty)=0$ for all $j$. Again we set $\hbar=1$.

We now consider the experimental dynamic observables.

(a) The excited state total population probability $P(t)$. The population probability of the entire Rydberg manifold is

$$P(t)=\sum_j |\langle j|\Psi(t)\rangle|^2. \tag{A3}$$

Equations (A2) and (A3) result in

$$P(t)=\sum_j |C_j(t)|^2. \tag{A4}$$

(b) The population probability $I(t)$ of the doorway state $|s\rangle$, which is given by

$$I(t)=|\langle s|\Psi(t)\rangle|^2, \tag{A5}$$

which, together with Eqs. (A2) and (3.2) gives

$$I(t)=\left|\sum_j C_j(t)a_s^{(j)*}\right|^2. \tag{A6}$$

To obtain explicit expressions for the population probabilities $P(t)$, Eq. (A4), and $I(t)$, Eq. (A6), we utilize the time dependent Schrödinger equation for the equations of motion for amplitudes (at the time domain $0\leqslant t'\leqslant t$). For weak exciting electromagnetic fields the equations of motion within the rotating wave approximation yield

$$\begin{aligned} i\dot{C}_g(t) &= \sum_j \mu_{gj}\epsilon_0^*(t)\ \exp[i(-E_j+\bar{E})t]C_j(t), \\ i\dot{C}_j(t) &= \mu_{jg}\epsilon_0(t)\ \exp[i(-E_j-\bar{E})t]C_g(t)-\frac{i\gamma_j}{2}C_j(t), \end{aligned} \tag{A7}$$

where $\mu_{gj}=\langle g|\hat{\mu}|j\rangle$ is the transition moment from $|g\rangle$ to $|j\rangle$, and according to Eq. (3.2), $\mu_{gj}=a_j^{(s)}\mu_{gs}$.

The solution of Eq. (A7) for weak fields is readily obtained by setting $C_g(t)=1$ for all $t$ in the equations of motion for $\{C_j(t)\}$, which results in

$$iC_j(t)=\mu_{gj}\ \exp(iE_j t)\int_{-\infty}^{t} d\tau\epsilon(\tau)f_j(t-\tau), \tag{A8}$$

where $\epsilon(\tau)=\epsilon_0(t)\ \exp(i\bar{E}t)$ and

$$f_j(x)=\exp[-iE_j x-(\gamma_j/2)x]. \tag{A9}$$

Equations (A4) and (A6) together with Eqs. (A8) and (A9) provide explicit expressions for the observables. In this procedure the product of $\epsilon^*(\tau)\epsilon(\tau')$ is replaced by the appropriate correlation function, Eq. (A1).

[1] (a) M. Bixon and J. Jortner, J. Chem. Phys. **48**, 715 (1968); (b) Mol. Cryst. **213**, 237 (1969); (c) Isr. J. Chem. **1**, 189 (1969).
[2] J. Jortner, J. Chim. Phys. (special issue) *Transitions Non Radiatives Dans Les Molécules* 9 (1969).
[3] J. Jortner and S. Leach, J. Chim. Phys. **77**, 7 (1980); **77**, 43 (1980).
[4] J. Jortner and G. C. Morris, J. Chem. Phys. **51**, 3689 (1969).
[5] A. Amirav and J. Jortner (to be published).
[6] R. L. Whetten, S. G. Grubb, C. E. Otis, A. C. Albrecht, and E. R. Grant, J. Chem. Phys. **82**, 1115 (1985).
[7] A. Amirav and J. Jortner, J. Chem. Phys. **82**, 4378 (1985).
[8] (a) R. S. Berry, J. Chem. Phys. **45**, 1228 (1966); (b) N. Bradsley, Chem. Phys. Lett. **1**, 229 (1967).
[9] A. Russek, M. R. Patterson, and R. L. Becker, Phys. Rev. **167**, 167 (1967).
[10] G. Herzberg and C. Jungen, J. Mol. Spectrosc. **41**, 425 (1992).
[11] C. Jungen and D. Dill, J. Chem. Phys. **73**, 3338 (1980).
[12] R. S. Mulliken, J. Am. Chem. Soc. **91**, 4615 (1969).
[13] M. Rault and C. Jungen, J. Chem. Phys. **74**, 3388 (1981).
[14] H. Lefebvre-Brion and R. W. Field, *Perturbations in the Spectra of Diatomic Molecules* (Academic, Orlando, 1986).
[15] U. Even, R. D. Levine, and R. Bersohn, J. Phys. Chem. **98**, 3472 (1994).
[16] D. Bahatt, U. Even, and R. D. Levine, J. Chem. Phys. **98**, 1744 (1993).
[17] U. Even, M. Ben-Nun, and R. D. Levine, Chem. Phys. Lett. **210**, 416 (1993).
[18] X. Zhang, J. M. Smith, and J. L. Knee, J. Chem. Phys. **99**, 3133 (1993).
[19] (a) K. Müller-Dethlefs, M. Sander, and E. W. Schlag, Chem. Phys. Lett. **112**, 291 (1984); (b) Z. Naturforsch. **38A**, 1089 (1984); (c) G. Reiser, W. Habenicht, K. Müller-Dethlefs, and E. W. Schlag, Chem. Phys. Lett. **152**, 119 (1988); (d) K. Müller-Dethlefs and E. W. Schlag, Annu. Rev. Phys. Chem. **42**, 109 (1991); (e) W. G. Scherzer, H. L. Selzle, E. W. Schlag, and

R. D. Levine, Phys. Rev. Lett. **72**, 1435 (1994); (f) Z. Naturforsch. **48A**, 1256 (1993).
[20] F. Merkt and T. P. Softley, Int. Rev. Phys. Chem. **12**, 205 (1993).
[21] W. A. Chupka, J. Chem. Phys. **98**, 4520 (1993).
[22] W. A. Chupka, J. Chem. Phys. **99**, 5800 (1993).
[23] S. T. Pratt, J. Chem. Phys. **98**, 9241 (1993).
[24] F. Merkt, J. Chem. Phys. **100**, 2623 (1994).
[25] E. Rabani, L. Ya. Baranov, R. D. Levine, and U. Even, Chem. Phys. Lett. **221**, 473 (1994).
[26] E. Rabani, R. D. Levine, and U. Even, J. Phys. Chem. (in press).
[27] U. Fano, Phys. Rev. A **2**, 353 (1970).
[28] U. Fano, J. Opt. Soc. Am. **65**, 979 (1975).
[29] S. A. Rice, R. Hochstrasser, and J. Jortner, in *Advances in Photochemistry*, edited by B. O. Pitts and G. Hammond (Wiley, New York, 1969).
[30] S. Mukamel and J. Jortner, in *Proceedings of the First International Congress on Quantum Chemistry*, Menton, France, 1973, edited by R. Daudel and B. Pullman (Reidel, New York, 1974), pp. 145–209.
[31] S. Mukamel and J. Jortner, in *MTP International Review of Science*, edited by A. D. Buckingham and C. A. Coulson (Butterworth, London, 1976), Vol. 13, p. 327.
[32] S. Mukamel and J. Jortner, in *Excited States*, edited by E. C. Lim (Academic, New York, 1977), Vol. III, pp. 57–107.
[33] F. Merkt and R. N. Zare, J. Chem. Phys. **101**, 3495 (1994).
[34] C. Bordas, P. F. Brevet, M. Broyer, J. Chevaleyre, P. Labastie, and J. P. Perrot, Phys. Rev. Lett. **60**, 917 (1988).
[35] M. Bixon and J. Jortner, J. Chem. Phys. **50**, 3284 (1969).
[36] M. Bixon and J. Jortner, J. Chem. Phys. **50**, 4061 (1969).
[37] J. Kommandeur and J. Jortner, Chem. Phys. **28**, 273 (1978).
[38] R. D. Levine and J. Jortner, in *Advances in Chemical Physics*, edited by J. Jortner, R. D. Levine, and S. A. Rice (Wiley–Interscience, New York, 1981), Vol. 47, pp. 1–114.
[39] M. Bixon, Y. Dothan, and J. Jortner, Mol. Phys. **17**, 109 (1969).
[40] H. A. Bethe and E. E. Salpeter, *Quantum Mechanics of One- and Two-Electron Atoms* (Springer, Berlin, 1957).
[41] K. Radler and J. Berkowitz, J. Chem. Phys. **70**, 216 (1979).
[42] D. Klar, K. Harth, J. Ganz, T. Kraft, M. W. Ruf, H. Hotop, V. Tsemekhman, K. Tsemekhman, and M. Ya. Amusia, Z. Phys. D **23**, 101 (1992).
[43] A. ten Wolde, L. D. Noordam, A. Legendijk, and H. B. van Linden van den Heuvell, Phys. Rev. Lett. **61**, 2099 (1988).
[44] A. ten Wolde, L. D. Noordam, A. Legendijk, and H. B. van den Linden van den Heuvell, Phys. Rev. A **40**, 485 (1989).
[45] For an exceptional case in intramolecular dynamics of a doorway state being pushed below a bound continuum, quasicontinuum, or discrete manifold see M. Gelbart and J. Jortner, J. Chem. Phys. **54**, 2070 (1971).
[46] M. L. Zimmerman, M. G. Littman, M. M. Kash, and D. Kleppner, Phys. Rev. A **20**, 2251 (1979).